Hydrogen dynamics in $[Me(H_2O)_6](ClO_4)_2$ with Me=Mg, Mn, Fe, Ni, and Zn investigated with quasielastic neutron scattering

C. Nöldeke, B. Asmussen, and W. Press
Institut für Experimentelle und Angewandte Physik, Universität Kiel, 24098 Kiel, Germany

H. Büttner
TU Delft, Julianalaan 134, 2600 AA Delft, The Netherlands

G. Kearley
Interfacultair Reactor Instituut, TU Delft, Mekelweg 15, 2629 JB Delft, The Netherlands

R. E. Lechner and B. Rufflé
Hahn-Meitner-Institut, Glienicker Straße 100, 14109 Berlin, Germany

The hydrogen dynamics in the metalhexahydrateperchlorates with Mg, Mn, Fe, Ni, and Zn as metal ions has been investigated with quasielastic neutron scattering. The water molecules perform 180°-flip motions on a picosecond time scale through a series of solid–solid phase transitions. In the highest temperature phase I and the subsequent phase II, rotational barriers of typically $E_a = 50$ meV are found. These values are surprisingly small in view of the low symmetry of H_2O molecules. The I → II phase transition has only very small effects on the hydrogen dynamics. At the transition into phase III an increase of the rotational barriers to typically $E_a = 250$ meV is found. This is interpreted as the formation of weak hydrogen bonds. In phase I 180°-flip motions provide a complete description of the observed data. In phases II and III an extension of the dynamical model toward a stronger localization of hydrogen is required. A preference is given to a mechanism leading to a temporary blockade of the flip motions. In phase III of the Fe compound, the existence of crystallographically different sites for water molecules is inferred. © *2000 American Institute of Physics.* [S0021-9606(00)01632-9]

I. INTRODUCTION

The rotational dynamics of small molecular entities in molecular crystals has been intensively studied over many years. Especially the connection between the dynamics and phase transitions in the crystalline state stays in focus. Thoroughly investigated examples for the different types of motion of a uniaxial rotor in molecular crystals are the hexaammine compounds $[Me(NH_3)_6]X_2$.[1–6] They usually have face-centered-cubic high temperature phases with rapid reorientations of the orientationally disordered ammonia. On cooling, these motions slow down and phase transitions may lead to low temperature phases with ordered NH_3.

In general orientational potentials are weak due to the high symmetry of NH_3. For groups of lower symmetry as H_2O they are expected to be considerably higher. Much less work has been done on the dynamics of the corresponding hexahydrate compounds $[Me(H_2O)_6]X_2$. In this article we present a systematic study of the H_2O dynamics in metal-hexahydrateperchlorates (MeHP).

A common feature of these $[Me(H_2O)_6](ClO_4)_2$ compounds is a basically hexagonal arrangement of the water and perchlorate molecules (Fig. 1).[7–10] The H_2O molecules lie in planes perpendicular to the *c*-axis of the crystal.[11] Their oxygen atoms form nearly perfect octahedra around the central metal ions.

All six substances undergo a series of structural solid–solid phase transitions (Table I), which are attributed to

slight changes in the water perchlorate arrangement and dynamics.[8–51] The close structural similarities between these substances allow for a systematic study of the effects of cation substitution on the local potentials. With its selective sensitivity for hydrogen dynamics, quasielastic neutron scattering (QNS) is ideally suited for this undertaking. MgHP and NiHP have been investigated with QNS in the past. Applying a scattering function for 180°-reorientations of H_2O groups, activation energies $E_a = 140$ meV (Ref. 48) and $E_a = 300$ meV (Ref. 33) were found with no apparent effect of the phase transitions I → II and II → III. Furthermore NMR studies of ZnHP and MgHP provided information about hydrogen dynamics and corresponding activation energies. Tumbling motions of the $Me(H_2O)_6$ complex were detected[13] with $E_a = 1000$ meV for ZnHP (Ref. 49) and $E_a = 520$ meV for MgHP.[48] For the water flip motion in ZnHP, $E_a = 170$ meV was found.[49]

The temperatures reported for the phase transitions vary considerably with the applied experimental method. Differences up to 25 K are found in the literature. Known causes for this are effects of thermal history, hysteresis, use of dopants, and supercooling. In some cases the existence of a phase transition is disputed.[10,15] We consider the results of calorimetric methods to be most reliable. Therefore the following discussion is based on those values. This article focuses on the water ligand dynamics and thus the information of noncalorimetric experiments must also be taken into ac-
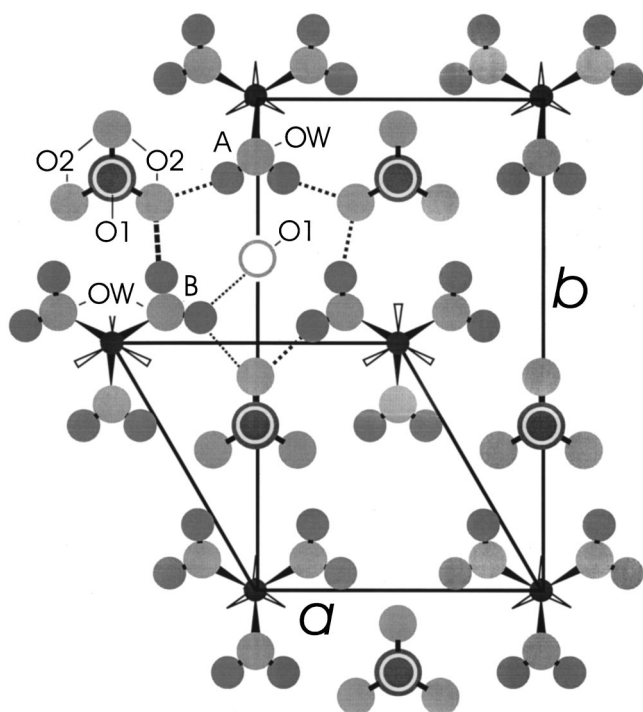
FIG. 1. Schematic view of the crystal structure of $[Me(H_2O)_6](ClO_4)_2$ (MeHP). The coordinates for the atoms are taken from Ref. 10. For clarity only selected atoms are shown. Mainly a layer approximately within $\pm c/4$ is presented. Therefore only three of the six water molecules (OW) around a metal ion are depicted. For the same reason only every second ClO_4^- group is shown, with O1 above the layer. O1 of the remaining ClO_4^- groups is within the layer (indicated once). Two different cells are marked, a small hexagonal and the corresponding orthorhombic pseudohexagonal cell with $b = \sqrt{3}a$. The cell doubling is required only by the metal atom positions. For the metal atoms on the corners of the orthorhombic cell $z_{Me} = -c/4$ holds and $z_{Me} = +c/4$ for those at the center. The hexagonal arrangement of water and perchlorate is basically maintained through a series of structural phase transitions. Hydrogen positions are calculated using $d_{O-H} = 0.96$ Å, $\alpha_{H-O-H} = 104°$, and $z_O = z_H = 0.023$ Å. For the perchlorate $z_{O2} = -0.46$ Å. The dotted lines mark selected hydrogen bonds. Water molecules marked with A and B visualize the symmetric and asymmetric configuration, which is discussed in Sec. III A.

TABLE I. Phase transition temperatures for MeHP as determined from calorimetric experiments.

Substance	I → II	II → III	III → IV
MgHP	324 K,[a] 325 K[a,b,c]	273 K[b,c]	168 K[b]
MnHP	323 K[a]	247 K[a]	134 K[d]
FeHP	337 K[a]	247 K,[a] 237 K[d]	
NiHP	360 K,[a] 361 K[e]	310 K[a,e]	
ZnHP	348 K,[f] 349 K[g]	290 K[f,g]	226 K[f]

[a]Reference 37.   [e]Reference 44.
[b]Reference 36.   [f]Reference 35.
[c]Reference 50.   [g]Reference 51.
[d]Reference 47.

MeHP with Me = Mg, Mn, Fe, Ni, and Zn. A short description of the experimental procedure is followed by a data interpretation in two steps. At first the type of hydrogen motion is identified and subsequently the corresponding activation energies are determined. While our results are in general agreement with previous work, some differences to earlier QNS experiments are noted. The sixth substance out of this series of isomorphs, CoHP, is not presented here. Details about structure and dynamics will be given elsewhere.[52]

II. EXPERIMENTAL DETAILS

The substances were obtained from Sigma-Aldrich. To avoid water intake they were stored and processed under argon atmosphere. As our original FeHP sample appeared moist, it was dried by keeping it in an extra container partially filled with silica. Approximately 1 g of each sample was ground and filled into aluminum containers with a $60 \times 30 \times 0.3$ mm^3 slab geometry. The containers were sealed before removal from the argon atmosphere.

The instruments NEAT[53,54] at the Hahn-Meitner-Institut, Berlin, and IN5 (Refs. 55,56) at the Institut Laue-Langevin, Grenoble, were used for the experiments. Unless otherwise noted the instruments were set to $\lambda = 5.1$ Å and a resolution of 0.09 MeV full width at half maximum (FWHM).

In a first step of data treatment the spectra of those detectors, which were contaminated by Bragg reflections or excessive noise were eliminated. Subsequent data reduction was performed with the program INX,[57] which includes corrections for scattering of the sample container and self-attenuation for a sample with slab geometry. As a result for each sample and each temperature a set of spectra at 15 different scattering angles was obtained from the NEAT data. From the IN5 data 14 groups were assembled; in case of the measurements at $\lambda = 6.5$ Å the number was reduced to 6 to ensure sufficient statistics.

III. RESULTS AND DISCUSSION

A. Identification of the type of hydrogen motion

Figure 2 shows as an example three quasielastic spectra of ZnHP obtained at $T = 280$ K for three selected angular groups marked by the corresponding values of wave vector transfer Q. A first inspection showed that an adequate analytical description is rather simple. Only the data of FeHP at $T = 237$ K and $T = 243$ K require a different treatment and are discussed separately. For one sample at a given temperature all n spectra can be described by

count. As long as there is an obvious correspondence between the phases observed with different methods, we apply the notation used in Table I.

Unfortunately, the information about details of the structures, especially hydrogen positions, is scarce. Starting with the hexagonal arrangement of water and perchlorate ions, typical unit cell parameters are $a \approx 7.8$ Å and $c \approx 5.2$ Å. With the positions of the metal ions taken into account, the orthorhombic space group $Pmn2_1$ with two formula units in the unit cell ($Z = 2$) and the pseudohexagonal axis ratio $b = \sqrt{3}a$ is assigned to the room temperature phases. Furthermore the metal ion arrangement is subject to a peculiar type of threefold twinning.[7] Only for the room temperature phase of ZnHP an x-ray single crystal structure refinement has been published.[10] Several observations obtained with a variety of experimental methods were explained in terms of crystallographically inequivalent sites for the water molecules. The conclusions concerning space group and unit cell are still controversial.

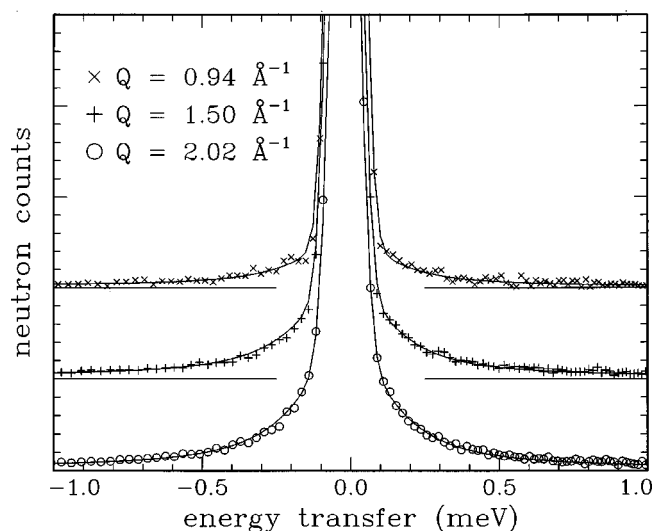In the following sections we present our results on

FIG. 2. Quasielastic scattering from ZnHP at $T = 280$ K. Three out of 15 spectra are shown. The lines were calculated using Eq. (1). For clarity the $Q = 0.94$ Å^{-1} and $Q = 1.50$ Å^{-1} data are shown in an offset.
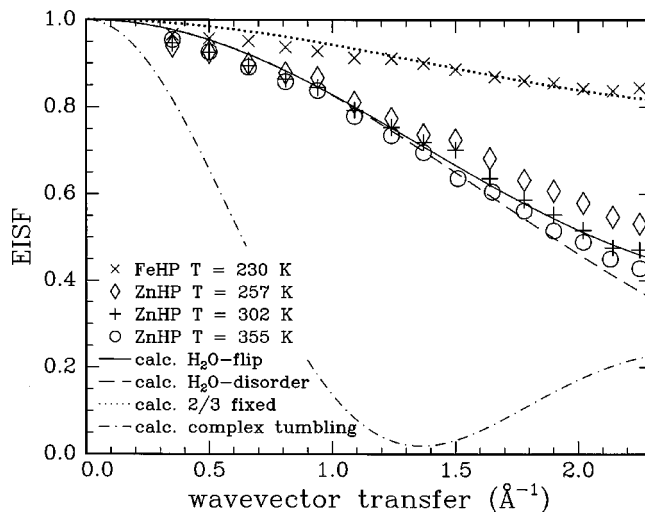

FIG. 3. The observed EISF of FeHP in phase III and of ZnHP in phases I, II, and III are shown. The data of FeHP in phase I and II, as well as those of MgHP, MnHP, and NiHP very closely resemble those of ZnHP in the corresponding phases. For $Q \lesssim 1.0$ Å^{-1} multiple scattering diminishes the observed values. Also four model calculations are presented. The H₂O 180°-flip motion provides the best agreement with the ZnHP data at $T = 355$ K and $T = 302$ K. This motion also describes the FeHP phase III data, if only 1/3 of the water molecules contribute on a time scale accessible with the instrumental setup.

$$I(Q_n, \omega) = A_{0,n}\delta(\omega) + A_{1,n}\mathcal{L}(\omega, \Gamma) + B_n. \tag{1}$$

The different values of Q are marked with the index n, $\hbar\omega$ denotes the energy transfer. The components of the spectra are an elastic contribution ($\hbar\omega = 0$), a quasielastic contribution with the shape of a Lorentzian $\mathcal{L}(\omega, \Gamma)$ with Q-independent half width at half maximum (HWHM) Γ, centered at $\hbar\omega = 0$, and B_n a flat background attributed to phonon scattering. $I(Q_n, \omega)$ is convoluted with the instrumental resolution and the coefficients $A_{0,n}$, $A_{1,n}$, B_n, and Γ are determined by a least squares procedure. An example of the thus calculated intensity $I(Q_n, \omega)$ is also shown in Fig. 2.

The observed elastic incoherent structure factor (EISF),[58,59] is determined via

$$\text{EISF}(Q_n) = \frac{A_{0,n}}{A_{0,n} + A_{1,n}}.$$

It contains the averaged information about the time averaged probability density distribution of the individual hydrogen atoms. Figure 3 shows the observed EISF for ZnHP and FeHP. Also the calculation for a hydrogen jump between two equivalent sites $d = 1.52$ Å apart (i.e., 180°-flips of the H₂O molecules about their twofold symmetry axis),[58]

$$\text{EISF}(Q) = \frac{1}{2} + \frac{\sin(Qd)}{2Qd} \tag{2}$$

is presented. The general agreement between measurement and calculation is very good. In Fig. 3 two further calculations for the EISF are shown

(i) The dash-dotted line is calculated for a jump process between six sites placed on the vertices of a regular octahedron. This is a simple approximation to a tumbling motion of the whole Me(H₂O)₆ complex. Obviously motions with such a large spatial extent are in disagreement with the data. There is no contradiction between our results and the reported observation of tumbling motions of the Me(H₂O)₆ complex in

NMR experiments (ZnHP;[13,49] MgHP),[48] as these motions are far too slow to be detected by QNS with our experimental setup.

(ii) The dashed line is calculated for a water molecule performing a diffusive rotational motion about its symmetry axis. This leads to a continuous density distribution on a circle and would be a signature of orientational disorder. A model which reduces this hydrogen distribution on a circle to four sites placed at equal distances on this circle (i.e., 90°-jumps), produces nearly the same EISF. The difference to the EISF of the 180°-reorientations becomes visible at larger values of momentum transfer Q. Although this difference is not large, the data clearly favor the 180°-flip model.

Deviations of the observed EISF from the calculation originate from three sources

(i) due to multiple scattering, at small Q the observed values are smaller than calculated.

(ii) In some cases a significant increase of the elastic intensity is observed for discrete values of Q. This is due to the incomplete removal of Bragg reflections in the first step of data reduction.

(iii) With decreasing temperature, the observed values become larger than the calculation for $Q \gtrsim 1.1$ Å^{-1}. This is an indication, that the 180°-flip model requires slight modifications which reduce the averaged available space of a hydrogen atom. A similar tendency was observed in [Ni(NH₃)₆](NO₃)₂ and [Mg(NH₃)₆](NO₃)₂.[4,6] The data of FeHP in phase III ($T = 230$ K, Fig. 3) show this effect in an extreme way. Obviously the simple flip model does not fit here. These data are therefore discussed separately at the end of this section.

One version of a modified flip model adapts the calculated EISF by decreasing the jump distance d in Eq. (2). In

TABLE II. Activation energies E_a for H$_2$O-flip motions. The second row gives the ranges for the parameter f denoting the deviation of the observed EISF from Eq. (2). Only values from NEAT experiments are given, as the values obtained from the IN5 data appeared to be biased, probably due to an overcompensation of the sample container scattering. For MnHP the drop from $f = 0.04$ to $f = 0.09$ occurs between $T = 343$ K and $T = 330$ K, which is above the I → II transition temperature $T = 323$ K given in Table I. The drop coincides with the transition temperature $T = 341$ K obtained from changes of infrared spectra.[a]

Substance		Phase I	Phase II	Phase III
MgHP	E_a	43 (3) meV		185 (15) meV
	f	0.01–0.02	0.06–0.07	0.12–0.19
MnHP	E_a	61 (1) meV		251 (3) meV
	f	0.03–0.04	0.09–0.12	0.17–0.22
FeHP	E_a	37 (1) meV		
	f	0.01–0.03	0.08–0.17	0.67
NiHP	E_a	65 (4) meV		290 (50) meV
	f	0.00	0.04	0.08–0.14
ZnHP	E_a	58 (3) meV		280 (20) meV
	f	0.00–0.03	0.04–0.07	0.08–0.11

[a]Reference 41.

Sec. III B values as small as $d = 1.25$ Å are obtained this way. In the picture of a 180°-flip motion this requires a considerable distortion of the water molecule geometry with changes in bond length or bond angle which make this explanation rather improbable.

Another modification is based on the assumption, that a small fraction f of the water molecules contributes to the elastic scattering only. The quasielastic scattering is produced by the remaining $1-f$ molecules. An interpretation of the increase of f with decreasing temperature may be attempted in terms of inequivalent sites for the water molecules. If f molecules occupy sites with strong orientational potentials this results in very long correlation times. Then the quasielastic scattering from these molecules cannot be distinguished from elastic scattering due to the finite instrumental resolution.

The values of f are obtained in Sec. III B (Table II). In phase I it is found for all substances, that all water molecules participate in the motion ($f \approx 0$). Thus the 180°-flip model completely suffices to describe these results. In phase II, $f = \frac{1}{24} \approx 0.04$ or $f = \frac{1}{12} \approx 0.08$ would require one out of 24 or one out of 12 molecules not to contribute to the quasielastic scattering. This is incompatible with space group $Pmn2_1$ and $Z = 2$. Therefore we propose a different explanation for the deviation of the observed EISF from Eq. (1).

This is obtained from a reinterpretation of f. The proposed standard configuration for a water molecule is symmetric and marked A in Fig. 1. Two hydrogen bonds are formed to the neighboring perchlorate ions. As the bond angle of H–OW–H = 104° differs from the angle O2–OW–O2 = 128° between the oxygen atoms, none of the two hydrogen bonds possesses the optimal linear arrangement. In configuration A the water molecules perform the 180°-flip motion. The alternative asymmetric configuration is marked B in Fig. 1. A 12° rotation about the z-axis will thus strengthen one of the bonds, while weakening the other at the same time. If the strengthened bond remains intact for times longer than 10^{-10} s the scattering of the corresponding

hydrogen will be observed as purely elastic. Via reorientation around this bond axis the other hydrogen may find further potential minima in direction of the two different O1 of the stacked perchlorate ions. The coefficient f is now taken as a measure of the time fraction each molecule spends in configuration B instead of A. If for simplicity it is assumed that jump distances and correlation times are similar for this type of motion and the 180°-flip motion, the fraction in time f' a molecule performs this additional type of motion can be calculated by $f' = 2f$ as only one hydrogen is immobile.

Summarizing, the difference between the observed EISF and Eq. (2) is taken as an indication of the existence of an alternative motion besides the dominating 180°-flip motion. From the present data alone, it is not possible to get more information.

For the data of FeHP in phase III, a model which assumes two crystallographic inequivalent sites with $f = 2/3$ provides a satisfactory description (Fig. 3). The existence of at least two inequivalent sites per unit cell for water molecules in FeHP phase III is supported by crystallographic results.[9] In this phase the hexagonal symmetry of the water perchlorate arrangement no longer exists and is reduced to orthorhombic. Further support comes from the observation of much slower hydrogen motions ($\Gamma \approx 5$ μeV) with the backscattering method.[52] These may account for the fraction which appears to be at rest in the present data. For the data obtained at IN5 at $T = 237$ K and $T = 243$ K a slight improvement of the fit is achieved, if an additional very narrow Lorentzian is used to model the slow process. Therefore the existence of at least two different sites for water molecules is obvious. Data from an EPR study were interpreted in terms of two coexisting phases in the temperature range 242 K $\geq T \geq 232$ K.[24] The present data do not allow us to distinguish between the two interpretations.

B. Correlation times and activation energies

The next step of data analysis focuses on the extraction of numerical values for correlation times $\tau \sim \Gamma^{-1}$. To achieve most reliable values, data for $Q \leq 0.85$ Å^{-1} are discarded as they carry little information and are contaminated by multiple scattering. To reduce the number of independent parameters the ratio of elastic and quasielastic intensities is fixed to

$$\frac{A_{0,n}}{A_{1,n}} = \frac{\text{EISF}(Q_n)}{1 - \text{EISF}(Q_n)},$$

with $\text{EISF}(Q_n)$ obtained from Eq. (2). Taking into account f as discussed in the preceding section, the model function

$$I(Q_n, \omega) = S_n\{[f + (1-f)\text{EISF}(Q_n)]\delta(\omega)$$
$$+ (1-f)(1 - \text{EISF}(Q_n))\mathcal{L}(\omega, \Gamma)\} + B_n \quad (3)$$

is used to determine Γ and f. S_n is a scale factor. In six spectra a Bragg reflection necessitated one additional parameter.

A summary of the values obtained for the parameter f is given in Table II. Varying the jump distance d instead of f gave slightly higher values of χ^2 and practically identical
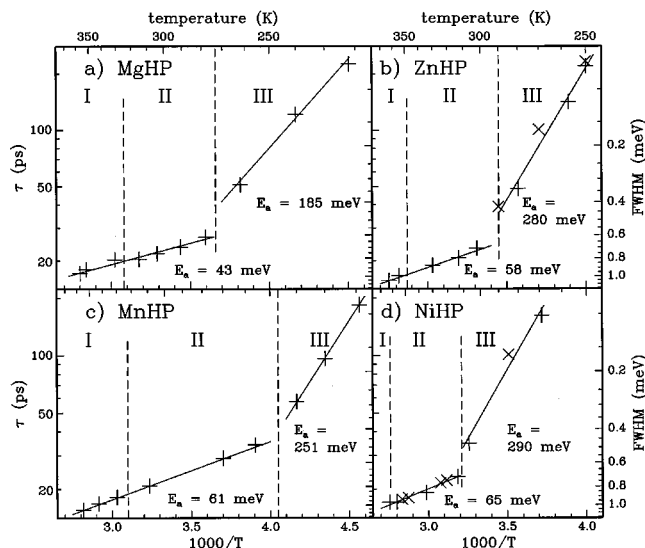
J. Chem. Phys., Vol. 113, No. 8, 22 August 2000

Hydrogen dynamics in $[Me(H_2O)_6](ClO_4)_2$ 3223

FIG. 4. Arrhenius plots of the correlation times τ for the H_2O flip motion in MeHP with Me=Mg [Fig. 4(a)], Zn [Fig. 4(b)], Mn [Fig. 4(c)], and Ni [Fig. 4(d)]. The dashed vertical lines denote the temperatures of the phase transitions (Table I). Data obtained on the instrument NEAT are marked by + and data obtained on IN5 are marked by ×. The size of the symbols is chosen to present an upper limit for the estimated error of the quasielastic linewidths. The IN5 data on ZnHP were obtained with a resolution width FWHM = 0.045 meV. The activation energies E_a are determined from the slope of the continuous lines.

values of Γ. The parameters d and f are strongly correlated and cannot be determined independently, therefore. Values obtained for d are 1.25 Å $\leqslant d \leqslant$ 1.52 Å.

For the phase III data of FeHP obtained on IN5 at T = 237 K and T = 243 K, no reliable correlation times can be given. As mentioned in the preceding section, a fit with two Lorentzians slightly improved the fit. The width of the narrow Lorentzian, which presents the slow motions, becomes smaller than the instrumental resolution and is therefore poorly defined. This also effects the correlated value of the broader component.

The widths Γ of the Lorentzians are inversely proportional to the mean residence time τ between two H_2O flips. Figure 4 presents the values of $\ln(\tau)$ vs T^{-1} for MgHP, MnHP, NiHP, and ZnHP. The comparison of values obtained from different experiments [Figs. 4(b) and 4(d)] gives a good impression of the reproducibility of the results. A simple Arrhenius behavior,

$$\tau = \tau_0 \exp\left(\frac{E_a}{k_B T}\right),$$

suffices to describe the data. The activation energies E_a, determined from the slopes of the straight lines are summarized in Table II. Within the data presented here, no effect of the transition I $\rightarrow$ II on E_a is found. E_a increases between 120 and 230 meV at the transition II $\rightarrow$ III.

C. The hindering potential in phase I and II

The values of the activation energies in phases I and II are remarkably small. The structural similarities of the substances and the absence of an observable effect of the I $\rightarrow$ II

transition on the activation energies are taken as guidelines in discussing the origin of the hindering potential for the water flip motion.

Investigations with x-ray powder diffraction have shown that the transition II $\rightarrow$ I is accompanied by an expansion of the crystallographic c-axis by $\Delta c \approx 0.1$ Å (ZnHP;[15] NiHP).[38] If the twofold screw axis (out-of-plane of Fig. 1) is retained during this expansion, as for ZnHP,[15] the z component of the O–O distances increases by $\Delta c/2$. This should result in a significant change of the interaction between neighboring water molecules. Since, however, E_a is basically unaffected by this transition, we conclude that the $H_2O–H_2O$ interaction gives only a minor contribution to the hindering potentials in phases I and II.

Another contribution to the hindering potential may arise from hydrogen bonds (Fig. 1). These should be weak due to the rather large O–O distance of 3 Å and the angle mismatch described above. For weak hydrogen bonds 150 meV is a typical bond energy value. For a 180° reorientation of an H_2O molecule with two hydrogen bonds one can expect E_a = 300 meV, five to seven times larger than the observed values. Therefore our results only can be understood if the hydrogen bonds are extremely weak. Further support for this conclusion comes from the fact that the I $\rightarrow$ II transition is associated with a change of perchlorate dynamics (MgHP;[12] NiHP;[28] MgHP, NiHP;[34] MgHP;[36] MnHP, FeHP).[37] This would involve breaking the hydrogen bonds and a corresponding change in E_a at this transition, contrary to our observation.

In MgHP the III $\rightarrow$ II transition was characterized by an increase of the disorder involving water.[51] This also conflicts with hydrogen bonding. Still a residual attraction of the partial charge of the hydrogen atoms by the perchlorate ions prevails and thus is a contribution to the hindering potential. A more detailed description of the water disorder is desirable, but requires additional structural information. The observed EISF provides some restrictions to the spatial extent of the hydrogen motions, as discussed above.

D. The hindering potential in phase III

Our data clearly show a marked effect of the II $\rightarrow$ III transition on the water ligand dynamics. This disagrees with the conclusions drawn from previous QNS experiments (MgHP;[48] NiHP).[33] However, upon closer inspection a change in activation energy might also be found in those data. The more pronounced effect in our results may be attributed to the advances in neutron spectroscopic instrumentation. The change of water ligand dynamics at this transition is also inferred from the isotope effect of H–D substitution. In a Mössbauer spectroscopy experiment with FeHP an increase of the phase transition temperature $\Delta T = 4$ K is reported.[16] $\Delta T = 3$ K was found for NiHP in a calorimetric study.[28]

As for the I $\rightarrow$ II transition, the structural and dynamical similarities of the five title compounds provide the guideline for the discussion. While the a- and c-axes of ZnHP show a marked change at this transition,[15] this is not the case for NiHP.[38] Therefore $H_2O–H_2O$ interactions can be ruled out as a source of the change in E_a. A general feature of the II $\rightarrow$

III transition is a symmetry reducing deformation of the water ligand octahedron (MgHP;[32] NiHP;[30] ZnHP;[31] MnHP).[41] This changes the H_2O–ClO_4 distances and may lead to the formation of hydrogen bonds. Further support comes from the observed increase in activation energy, which is in the range of weak hydrogen bonds.

IV. CONCLUSIONS

In the temperature range investigated for all five substances, a 180°-flip motion of the water molecules was found. The most prominent features are low energy barriers to this motion in the high temperature (I) and middle temperature (II) phases. The transition into the low temperature phase (III) is accompanied by a marked increase in the potential barrier. We propose the formation of hydrogen bonds between H_2O–ClO_4 as the source of the hindering potential to this motion in phase III with typical activation energies of 200 meV. At the transition III $\rightarrow$ II the reduction of activation energies to values around 50 meV indicates that hydrogen bonds, if still existing, become extremely weak. The phase transition II $\rightarrow$ I was not found to affect the hydrogen dynamics.

The spatial information obtained from the EISF clearly marks the 180°-flip motion as dominating process. Even in the high temperature phase I no indication for a free rotation was found. In this context the values of the hindering potentials in phases I and II are surprisingly small. The only effect of the II $\rightarrow$ I transition are slight changes of the EISF. The model we propose to explain these changes agrees with the change of perchlorate dynamics at this transition. Increased librations of the perchlorate in phase I decreases the stability of the strengthened bond in the asymmetric configuration, which reduces the probability of occurrence.

A tumbling of the $Me(H_2O)_6$ complex, as observed with NMR, is too slow to be detected in our experiments.

The activation energies in phases I and II do not show an obvious systematic link to other physical parameters of the different substances, such as transition temperatures. NiHP with the largest $E_a = 65$ meV has also the largest $T_{I \rightarrow II} = 360$ K. MnHP on the other hand has nearly the same $E_a = 61$ meV but the smallest $T_{I \rightarrow II} = 323$ K. The comparison of E_a with $T_{II \rightarrow III}$ gives similar results. Both, the activation energies in phase III and $T_{II \rightarrow III}$ decrease in the sequence NiHP, ZnHP, MnHP, but MgHP does not fit into this scheme.

Activation energies $E_a \approx 50$ meV for the water flip motions in MeHP in the high temperature phases are somewhat larger than $E_a \approx 20$ meV for NH_3 120°-reorientational jumps in the corresponding metalhexaammineperchlorates.[1,2] This agrees with the general expectation that hindering potentials decrease with increasing molecular symmetry.

[1] J. A. Janik, J. M. Janik, K. Otnes, and K. Rosciszewski, Physica B **83**, 259 (1976).
[2] J. A. Janik, J. M. Janik, A. Migdal-Mikuli, E. Mikuli, K. Ontes, and I. Svare, Physica B **97**, 47 (1979).
[3] G. J. Kearley and H. Blank, Can. J. Chem. **66**, 692 (1988).
[4] J. M. Janik, J. A. Janik, A. Migdal-Mikuli, E. Mikuli, and K. Ontes, Physica B **168**, 45 (1991).
[5] P. Schiebel, A. Hoser, W. Prandl, G. Heger, W. Paulus, and P. Schweiss, J. Phys.: Condens. Matter **6**, 10 989 (1994).
[6] A. Migdal-Mikuli and E. Mikuli, Acta Phys. Pol. A **88**, 527 (1995).
[7] C. D. West, Z. Kristallogr. **91A**, 480 (1935).
[8] M. Ghosh and S. Ray, Z. Kristallogr. **145**, 146 (1977).
[9] M. Ghosh and S. Ray, Z. Kristallogr. **155**, 129 (1981).
[10] S. Ghosh, M. Mukherjee, A. Seal, and S. Ray, Acta Crystallogr., Sect. B: Struct. Sci. **53**, 639 (1997).
[11] M. B. Patel, A. Agarwal, and H. D. Bist, J. Raman Spectrosc. **14**, 406 (1983).
[12] A. Agarwal, M. B. Patel, and H. D. Bist, J. Raman Spectrosc. **16**, 303 (1985).
[13] B. Borzecka, S. F. Sagnowski, and S. Hodorowicz, Phys. Status Solidi A **64**, 557 (1981).
[14] B. Borzecka and S. Hodorowicz, Acta Phys. Pol. A **63**, 385 (1983).
[15] B. Borzecka and S. Hodorowicz, Cryst. Res. Technol. **30**, 613 (1995).
[16] B. Brunot, Chem. Phys. Lett. **29**, 368 (1974).
[17] B. Chaudhuri, J. Phys. C **7**, 3962 (1974).
[18] B. Chaudhuri and D. Ghosh, Phys. Status Solidi A **23**, 649 (1974).
[19] B. Chaudhuri, Solid State Commun. **16**, 767 (1975).
[20] B. Chaudhuri, J. Phys. C **9**, 1285 (1976).
[21] J. M. D. Coey, I. Dezsi, P. M. Thomas, and P. J. Ouseph, Phys. Lett. A **41**, 125 (1972).
[22] R. Dayal, D. Ramachandra Rao, and P. Venkateswarlu, Can. J. Phys. **56**, 1175 (1978).
[23] R. Dayal, Indian J. Phys., A **53**, 514 (1979).
[24] R. Dayal, D. Ramachandra Rao, and P. Venkateswarlu, J. Magn. Reson. **36**, 99 (1979).
[25] I. Dezsi and L. Keszthelyi, Solid State Commun. **4**, 511 (1966).
[26] M. Falk, P. F. Seto, and M. A. White, J. Chem. Phys. **81**, 3752 (1984).
[27] M. Ghosh and S. Ray, Indian J. Phys. **48**, 1149 (1974).
[28] M. Godlewska and M. Rachwalska, J. Therm. Anal. **45**, 1073 (1995).
[29] A. K. Jain and G. C. Upreti, Solid State Commun. **28**, 571 (1978).
[30] A. K. Jain and G. C. Upreti, J. Phys. C **13**, 5177 (1980).
[31] A. K. Jain and G. C. Upreti, J. Phys. Chem. Solids **43**, 563 (1982).
[32] A. K. Jain and G. C. Upreti, J. Phys. Chem. Solids **44**, 549 (1983).
[33] J. A. Janik, J. M. Janik, K. Otnes, and T. Stanek, Acta Phys. Pol. A **59**, 815 (1981).
[34] J. M. Janik, A. Migdal-Mikuli, E. Mikuli, and T. Stanek, Acta Phys. Pol. A **59**, 599 (1981).
[35] A. Migdal-Mikuli, E. Mikuli, and J. Mayer, Mol. Mater. **9**, 205 (1997).
[36] E. Mikuli, A. Migdal-Mikuli, M. Rachwalska, and T. Stanek, Physica B **104**, 326 (1981).
[37] E. Mikuli, A. Migdal-Mikuli, and J. Mayer, Mol. Mater. **8**, 273 (1997).
[38] L. Novakovic, J. Dojcilovic, M. M. Napijalo, M. Lj Napijalo, D. Lazar, and B. Ribar, Solid State Commun. **70**, 1031 (1989).
[39] M. B. Patel and H. D. Bist, J. Phys. Colloq. **42** (Suppl. 12), C6-917 (1981).
[40] M. B. Patel and H. D. Bist, J. Chem. Phys. **76**, 6445 (1982).
[41] M. B. Patel, S. Patel, D. P. Khandelwal, and H. D. Bist, Chem. Phys. Lett. **101**, 93 (1983).
[42] M. B. Patel, J. Chem. Phys. **81**, 3753 (1984).
[43] M. B. Patel, Solid State Commun. **53**, 431 (1985).
[44] M. Rachwalska and T. Stanek, Phys. Status Solidi A **48**, 297 (1978).
[45] W. M. Reiff, R. B. Frankel, and C. R. Abeledo, Chem. Phys. Lett. **22**, 124 (1973).
[46] J. Sartorelli, S. Isotani, J. A. Ochi, W. Sano, and A. Piccini, Chem. Phys. Lett. **57**, 608 (1978).
[47] M. Sinha, A. Pal, and S. K. Dutta, J. Phys. C **9**, 2783 (1976).
[48] I. Svare, B. O. Fimland, K. Otnes, J. A. Janik, J. M. Janik, E. Mikuli, and A. Migdal-Mikuli, Physica B **106**, 195 (1981).
[49] I. Svare and B. O. Fimland, J. Chem. Phys. **74**, 5977 (1981).

[50] M. White, J. Chem. Thermodyn. **16**, 885 (1984).

[51] M. White and M. Falk, J. Chem. Phys. **84**, 3484 (1986).

[52] C. Nöldeke *et al.* (unpublished).

[53] R. E. Lechner, ICANS-XI, KEK Report 90-25, Natl. Lab. for High Energy Physics, Tsukuba, 1991, p. 717.

[54] R. E. Lechner, Neutron News **7**, 9 (1996).

[55] R. Scherm, Internal Report Jul-295-NP, KFA, Julich, Germany, 1965.

[56] R. E. Lechner, *Neutron Scattering in the Nineties* (IAEA, Vienna, 1985), pp. 401–407.

[57] F. Rieutord, ILL Internal Report, 1990.

[58] M. Bée, *Quasielastic Neutron Scattering* (Hilger, Bristol, 1988), and references therein.

[59] R. E. Lechner, in *Quasielastic Neutron Scattering*, edited by J. Colmenero, A. Alegria, and F. J. Bermejo (World Scientific, Singapore and London, 1994), pp. 62–92, and references therein.